Research Square

Preprints are preliminary reports that have not undergone peer review.
They should not be considered conclusive, used to inform clinical practice,
or referenced by the media as validated information.

A 3D-Printed Neural Probe with Geometry-Defined Lithography-Free Metallization and Parylene Encapsulation

Armin Sedighi

armin.sedighi@wayne.edu

Wayne State University https://orcid.org/0000-0001-8208-8672

Mehedi Hasan

Wayne State University https://orcid.org/0009-0002-0194-4575

Yong Xu

yongxu@wayne.edu

Wayne State University

Research Article

Keywords: two-photon polymerization, neural probe, additive manufacturing, Parylene-C, maskless metallization, bioelectronics

Posted Date: November 6th, 2026

DOI: https://doi.org/10.21203/rs.3.rs-11627269/v1

License: This work is licensed under a Creative Commons Attribution 4.0 International License.
Read Full License

Additional Declarations: The authors declare no competing interests.

Abstract

Two-photon polymerization enables neural probes with complex three-dimensional geometries, but selectively metallizing and insulating these structures remains challenging. We present a geometry-defined fabrication process that combines trench-guided metallization with vapor-deposited Parylene-C encapsulation and lithography-free electrode exposure. Re-entrant trenches guide line-of-sight Ti/Au evaporation to form electrically separated interconnects connected to electrode sites and contact pads. A conformal Parylene-C coating then seals the high-aspect-ratio trenches over the interconnects, and a timed, maskless O_2 plasma etch-back followed by SF_6/O_2 plasma treatment exposes the electrodes and pads while retaining insulation over the recessed interconnects. We fabricated a prototype comprising a 2 mm-long shank with four mushroom-shaped electrodes, each 15 μm in diameter. Scanning electron microscopy showed metal deposition at the trench bottoms, Parylene-C coverage, and selective electrode exposure after plasma processing. Electrochemical impedance spectroscopy in phosphate-buffered saline showed an impedance magnitude of approximately 1 MΩ at 1 kHz before and after insertion into 0.6% agarose gel. The probe reached a 2 mm insertion depth without observed buckling or fracture. These results demonstrate a fabrication proof of concept for 3D-printed neural probes using geometry-defined metallization and selective Parylene encapsulation, providing a potential route toward scalable fabrication of 3D-printed bioelectronic microsystems

1. Introduction

Penetrating neural probes are essential tools for investigating neural function and developing treatments for neurological disorders [1, 2]. By positioning electrodes within neural tissue, these devices enable localized recording and electrical stimulation, providing access to neural activity across different depths and anatomical regions. Their performance depends on both electrical characteristics and structural features, including shank dimensions, tip shape, and electrode placement. Conventional probes are fabricated by assembling microwires or by planar microfabrication in silicon or polymers. CMOS-based probes such as Neuropixels provide high channel counts [3], but planar fabrication constrains the three-dimensional geometry of individual shanks and electrode features. Realizing complex out-of-plane structures often requires additional processing or assembly, motivating alternative fabrication approaches.

Additive manufacturing provides greater freedom to tailor neural-interface geometries [4, 5]. In particular, two-photon polymerization (2PP) enables the fabrication of diverse three-dimensional features, including tapered tips and curved transitions, with micrometer or submicrometer spatial resolution. Recent work has paired 2PP-printed structures with thin-film metallization and Parylene-C insulation to build high-density neural interfaces. Brown *et al.* used Ti/Pt metallization patterned with a Cr lift-off mask, followed by Parylene-C encapsulation and laser opening of the electrode sites [6]. Wang *et al.* reported directly printed 3D electrodes using Ge-assisted lift-off, Parylene-C passivation, and plasma-based electrode exposure [7]. Other approaches avoid a metal-deposition step altogether, for example by pyrolyzing

printed polymer into carbon electrodes [8] or by printing from a conductive polymer [9], but the conductive material then cannot be selectively insulated within the same printed architecture.

Despite this progress, making an electrically functional 3D probe typically still requires several post-processing steps to define the conductive and insulated regions, such as lithographic patterning, lift-off, laser ablation, or plasma etching. Each step adds complexity, and together they slow design iteration, which is one of the main advantages of additive manufacturing. Maskless or lithography-free strategies for defining electrical function are therefore of significant interest.

We previously demonstrated a lithography-free geometry-defined fabrication process for a 2PP-printed, single-shank neural probe [10]. Re-entrant trenches with openings narrower than their bases guided line-of-sight Ti/Pt evaporation to define electrode sites, interconnects, and contact pads without a lithographic mask. A liquid SU-8 droplet wicked through the trenches by capillary action and stopped at convex electrode edges, insulating the traces while leaving the electrode surfaces exposed. The probe retained similar cyclic voltammetry and impedance responses after insertion into 0.6% agarose gel [10]. Although this approach defined both metallization and selective encapsulation through geometry, the achievable SU-8 wicking distance and applicability to longer or more complex pathways also remained to be established [10].

In this work, we keep the trench-guided metallization and replace the liquid-phase insulation step with vapor-phase Parylene-C deposition. Parylene-C is a conformal, biocompatible material that is widely used for bioelectronic devices [11]. However, it coats every exposed surface, so the electrodes and contact pads must be re-opened afterwards, which is normally achieved by laser ablation, lithographic masking, or plasma etching through a mask. We instead design the trenches so that Parylene self-seals over the traces at the bottom. The Parylene above the interconnects is then far thicker than on the electrodes and pads, and a timed, maskless O_2 plasma etch-back exposes only the electrodes and pads. This yields a maskless encapsulation and selective-exposure process in which conformal Parylene-C deposition and a timed etch-back replace liquid SU-8 wicking, with the trench geometry itself providing the etch selectivity between electrodes and interconnects. We demonstrate the approach using Ti/Au metallization on a 2 mm-long probe with four mushroom-shaped electrodes and characterize the structure by SEM, EIS in PBS, and insertion-force measurements in agarose gel.

2. Design and Fabrication Concept

The probe (Fig. 1) comprises a 2 mm-long shank with four mushroom-shaped electrodes, trench-defined interconnects, and contact pads. Ramps connect the recessed interconnects to the electrode heads. In the CAD design, the shank is approximately 50 µm wide and contains a re-entrant trench approximately 17 µm deep, with an opening width of 10 µm and a base width of 18 µm. The mushroom-shaped electrodes are 15 µm in diameter. Square-resistance test structures on the contact pads provide features for resistance measurements.

The process uses geometry to define both the conductive pathways and their selective insulation, as illustrated in Fig. 2. First, directional evaporation deposits metal onto the trench bottoms, electrode heads, and contact pads, while shadowed portions of the trench sidewalls remain uncoated. This discontinuity defines electrically separated conductive pathways without a mask, as we previously demonstrated [10]. Second, conformal Parylene-C deposition closes the narrow trench openings over the recessed traces. The resulting coating profile provides greater protection over the interconnects during plasma etching than over the electrode heads and pads. A timed blanket plasma etch can therefore expose the electrodes and pads while retaining insulation over the interconnects. Trench closure may leave an internal void; complete filling is not required, provided that a continuous Parylene barrier remains over the interconnects after etching.

3. Methods

3.1 Printing and base insulation

The probes were printed by 2PP with IP-S photoresist on a Nanoscribe Quantum X shape system with a 25× objective, using the shell-based writing strategy and block stitching described previously [10]. After printing, the samples were developed in propylene glycol monomethyl ether acetate (PGMEA), rinsed in isopropyl alcohol, and post-cured under UV light (~ 405 nm). A 1 μm Parylene-C base layer was then deposited (PDS 2035, Specialty Coating Systems) to isolate the resin from the biological environment, and it was treated briefly with O_2 plasma to improve metal adhesion.

3.2 Maskless metallization

Ti/Au layers with nominal thicknesses of 15 nm and 150 nm, respectively, were deposited by e-beam evaporation (Angstrom Engineering) at 2 Å/s for each layer. The re-entrant trench geometry defined the conductive pathways without lithographic patterning. The present probes used Au rather than the Pt employed in our previous work [10].

3.3 Encapsulation and maskless electrode exposure

A second, 7 μm-thick Parylene-C layer was deposited conformally over all surfaces. This layer encapsulated the metal traces by self-sealing of the high-aspect-ratio trenches. A timed, maskless O_2 plasma etch-back was performed using a PlasmaTherm 790 system RF power 105 W, chamber pressure 100 mTorr, O_2 flow 99 sccm, etch time 40 min) removed the surface Parylene from the electrodes and contact pads while preserving insulation over the recessed interconnects. A subsequent SF_6/O_2 plasma treatment (SF_6: 6 sccm; O_2: 60 sccm; RF power: 50 W; duration: 20 min) was used to remove residual material from the electrode surfaces.

3.4 Characterization

The device was imaged by scanning electron microscopy (SEM) at each process stage, and a cross-section of a trench-defined interconnect was imaged after metallization. Electrochemical impedance

spectroscopy (EIS) was performed in 1× phosphate-buffered saline (PBS) using a PalmSens4 potentiostat in a three-electrode configuration, with an Ag/AgCl reference electrode, a Pt mesh counter electrode, and the probe as the working electrode. Spectra were acquired from 0.1 Hz to 50 kHz at 0.0 V DC with a 50 mV AC perturbation. Mechanical insertion was performed in 0.6% agarose gel to a depth of 2 mm. The probe was mounted on a 10 g load cell while the gel was advanced by a syringe pump at 2 mm/min, as described previously [10], and the insertion force was recorded. EIS was measured before and after insertion.

4. Results and Discussion

4.1 Maskless metallization

Figure 3 shows the probe after Ti/Au metallization. The needle-shaped tip, the shank, and the trenches that route the interconnects along it remain well defined after the evaporation, and the electrode sites are visible along the shank. The inset shows a mushroom-shaped electrode connected to a recessed trace by a ramp, which provides a continuous geometric pathway for metal deposition from the trench bottom to the electrode head. Electrical continuity across similar ramps was demonstrated in our previous work [10]. The cross-sectional SEM image in Fig. 4 shows metal at the trench bottoms beneath the re-entrant openings. This observation supports the geometry-defined deposition mechanism, although a single cross-section does not establish end-to-end trace continuity or interchannel isolation.

4.2 Parylene encapsulation and etch-back

Figure 5 shows the electrode region during encapsulation and exposure. After metallization, the electrode head and connecting ramp are visible within the open trench (Fig. 5a). Following deposition of the nominally 7 μm-thick Parylene-C coating, the trench opening appears sealed and the electrode is covered (Fig. 5b). Blanket O_2 plasma etch-back reveals the electrode region, with residual material visible around the opening (Fig. 5c). The subsequent SF_6/O_2 treatment produces a cleaner exposed electrode surface, while the surrounding Parylene-C coating remains over the interconnect region (Fig. 4d). These images support selective electrode exposure by the combined trench-sealing and plasma-etching process. The maskless exposure works because the interconnects sit at the bottoms of deep trenches, where the effective Parylene thickness above the metal is substantially greater than 7 μm. The same timed etch therefore clears the thinner coating on the electrodes while leaving the interconnects insulated.

4.3 Mechanical insertion

The probe was inserted into 0.6% agarose gel at 2 mm/min to evaluate penetration into a soft tissue phantom (Fig. 6). It reached a depth of 2 mm without observed buckling or fracture. The force remained near baseline until insertion began at approximately 67 s and then increased as the shank entered the gel, with a few small peaks early in the insertion. The force was 3.75 mN at the indicated 2 mm insertion

depth. The probe continued to advance for a short duration and halted at approximately 135 s, at which point the force reached a maximum of about 5.2 mN. During the following holding period (about 135 s to 165 s), the force decreased to roughly 2.2 mN, possibly due to stress relaxation of the viscoelastic gel. It returned to the baseline when the probe was retracted at about 165 s. Together with the unchanged impedance after insertion (Fig. 7), these results indicate that the probe withstands insertion into a brain-mimicking medium.

4.4 Electrochemical performance

The EIS spectra measured in PBS before and after agarose insertion show similar impedance magnitudes, including values of approximately 1 MΩ at 1 kHz (Fig. 7a). The phase responses exhibit frequency-dependent differences (Fig. 7b). These measurements support retention of the measured electrode's electrical response after insertion. However, similar impedance spectra alone do not establish complete preservation of the insulation or exclude leakage and interchannel coupling. Dedicated insulation and isolation measurements are needed to assess those properties in the future study.

.

4.5 Limitations and outlook

This study demonstrates fabrication and benchtop characterization of a prototype; neural recording and stimulation have not been evaluated. Small gold electrodes can exhibit high impedance [12], but recording suitability also depends on electrode noise, amplifier input impedance, and the intended signal bandwidth. Surface modification or a larger exposed area could reduce impedance. Long-term soaking, leakage-current measurements, interchannel isolation tests, and repeated insertion studies are needed to evaluate insulation stability and reproducibility. Agarose insertion does not establish performance in brain tissue or compatibility with meningeal penetration. Although Parylene-C is used in bioelectronic devices [11], the biocompatibility of the complete fabricated probe, including plasma-processed surfaces and any exposed resin, remains to be assessed. Multi-shank probes were not fabricated here. Vapor deposition and blanket etching may simplify processing of arrays by avoiding per-shank liquid dispensing, but coating uniformity, trench sealing, etch access, and line-of-sight metal shadowing must be verified for denser geometries. Changes to electrode count, spacing, or routing can be implemented in the printed design, subject to these fabrication constraints.

5. Conclusion

We demonstrated a 2PP-printed penetrating probe fabricated using trench-guided Ti/Au metallization, conformal Parylene-C encapsulation, and maskless plasma exposure of the electrode sites and contact pads. SEM confirmed selective metal deposition within the trenches, Parylene-C encapsulation, and lithography-free electrode exposure following plasma treatment. Impedance was stable before and after

insertion into agarose gel, and the 2 mm shank penetrated without structural failure. Because the Parylene deposition and etch-back act on all shanks at once, we expect this approach to scale to multi-shank probes and higher electrode counts more readily than liquid-phase encapsulation. By removing lithography from the metallization and encapsulation steps, this approach offers a scalable route toward functional 3D-printed bioelectronic microsystems.

Declarations

Acknowledgments

This material is based upon work supported in part by the National Science Foundation under MRI Award No. 2116715, “Acquisition of a Nanoscale 3D Printer for Fundamental and Applied Research.” Parylene coating, metal evaporation, and plasma processing were carried out at the Lurie Nanofabrication Facility at the University of Michigan.

References

1. Luan L et al (2023) Emerging penetrating neural electrodes: in pursuit of large scale and longevity. Annu Rev Biomed Eng 25:185–205
2. Normann RA, Fernandez E (2016) Clinical applications of penetrating neural interfaces and Utah Electrode Array technologies. J Neural Eng 13:061003
3. Steinmetz NA et al (2021) Neuropixels 2.0: a miniaturized high-density probe for stable, long-term brain recordings. Science 372:eabf4588
4. Saleh MS et al (2022) CMU array: a 3D nanoprinted, fully customizable high-density microelectrode array platform. Sci Adv 8:eabj4853
5. Parker KE et al (2023) Customizable, wireless and implantable neural probe design and fabrication via 3D printing. Nat Protoc 18:3–21
6. Brown MA et al (2023) Direct laser writing of 3D electrodes on flexible substrates. Nat Commun 14:3610
7. Wang P et al (2025) Direct-print 3D electrodes for large-scale, high-density, and customizable neural interfaces. Adv Sci 12:e2408602
8. Yang C et al (2018) 3D-printed carbon electrodes for neurotransmitter detection. Angew Chem Int Ed 57:14255–14259
9. Won S et al (2026) A customizable 3D-printed neural probe array using two-photon polymerization with millimeter-scaled conductive polymer as an electrode material. ACS Appl Mater Interfaces 18:32434–32445
10. Sedighi A, Hasan M, Feng X, Xu Y (2026) 3D-printed penetrating neural probes with maskless metallization and encapsulation. Addit Manuf Lett 18:100408. 10.1016/j.addlet.2026.100408

11. Chang TY et al (2007) Cell and protein compatibility of parylene-C surfaces. Langmuir 23:11718–11725
12. Fan B, Wolfrum B, Robinson JT (2021) Impedance scaling for gold and platinum microelectrodes. J Neural Eng 18:056025

Figures

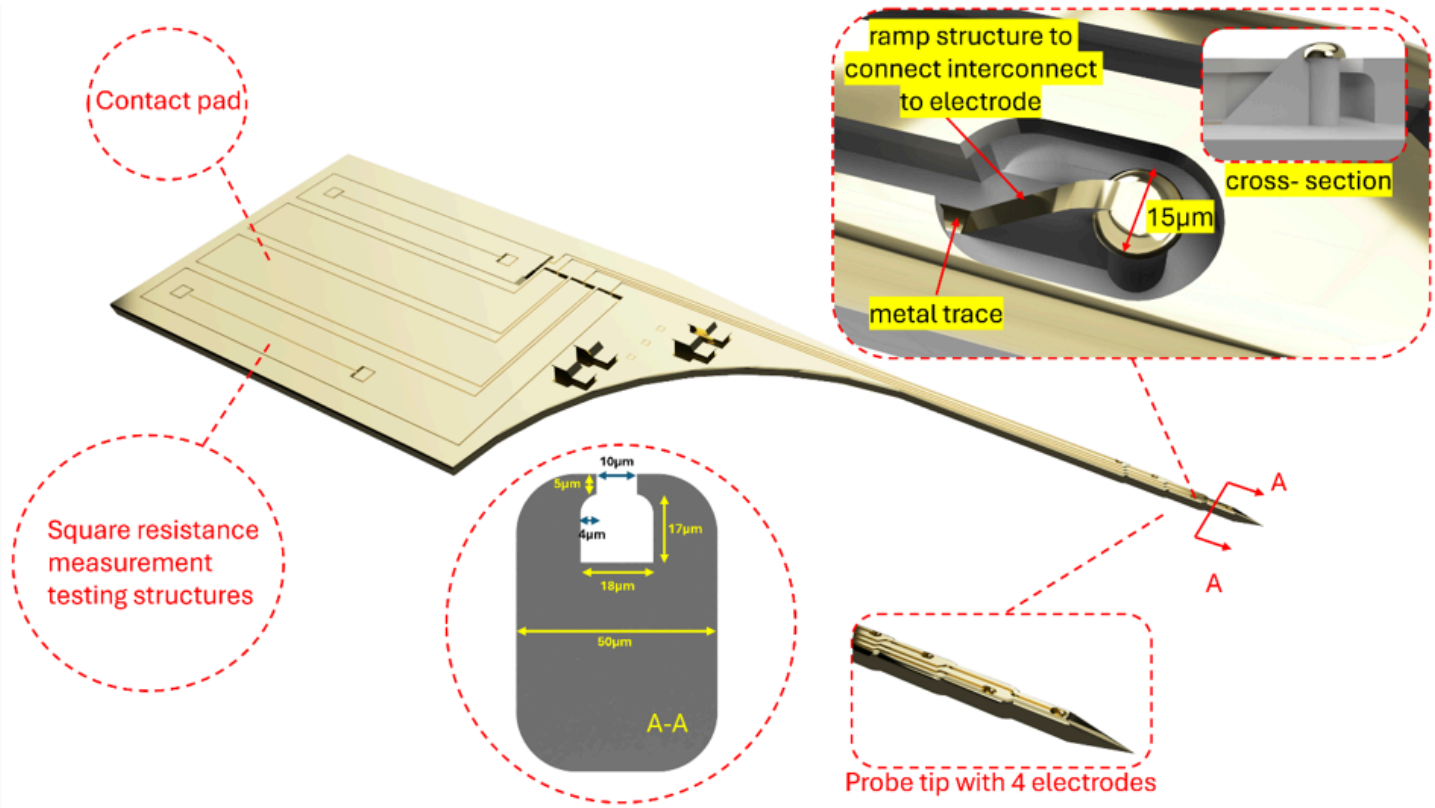


Figure 1

Probe architecture and key design features, showing the contact pads, square resistance-measurement test structures, probe tip with four electrodes, a cross-section of the shank (A–A), and a detail of the ramp structure connecting the metal trace to a mushroom-shaped electrode.

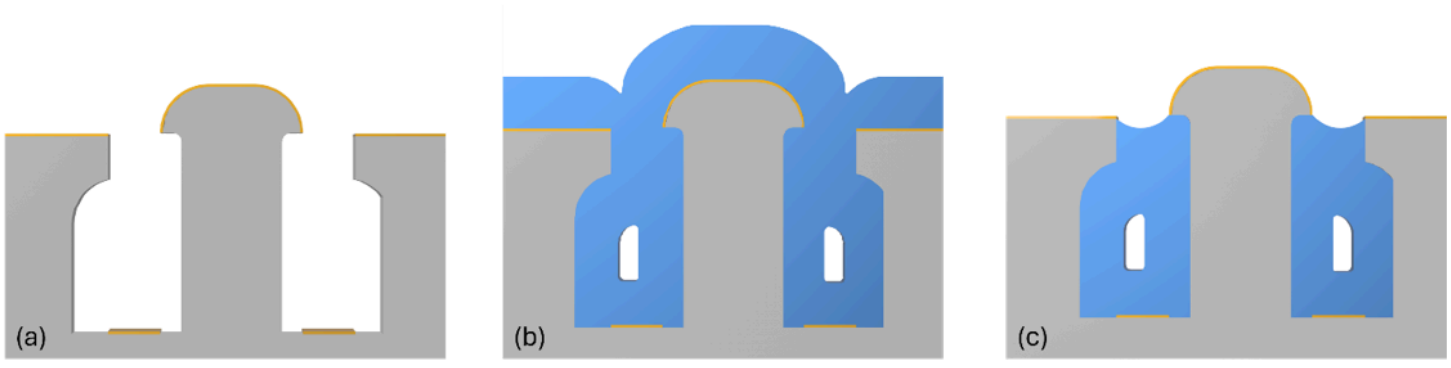


Figure 2

Schematic cross-sectional views of the probe shank illustrating geometry-assisted, lithography-free metallization and selective encapsulation by conformal Parylene-C deposition and plasma etch-back: (a) after metal evaporation; (b) after conformal Parylene-C deposition; and (c) after timed, blanket O_2 plasma etching. Gray, yellow, and blue represent the printed structure, metal, and Parylene-C, respectively. Schematics are not to scale.

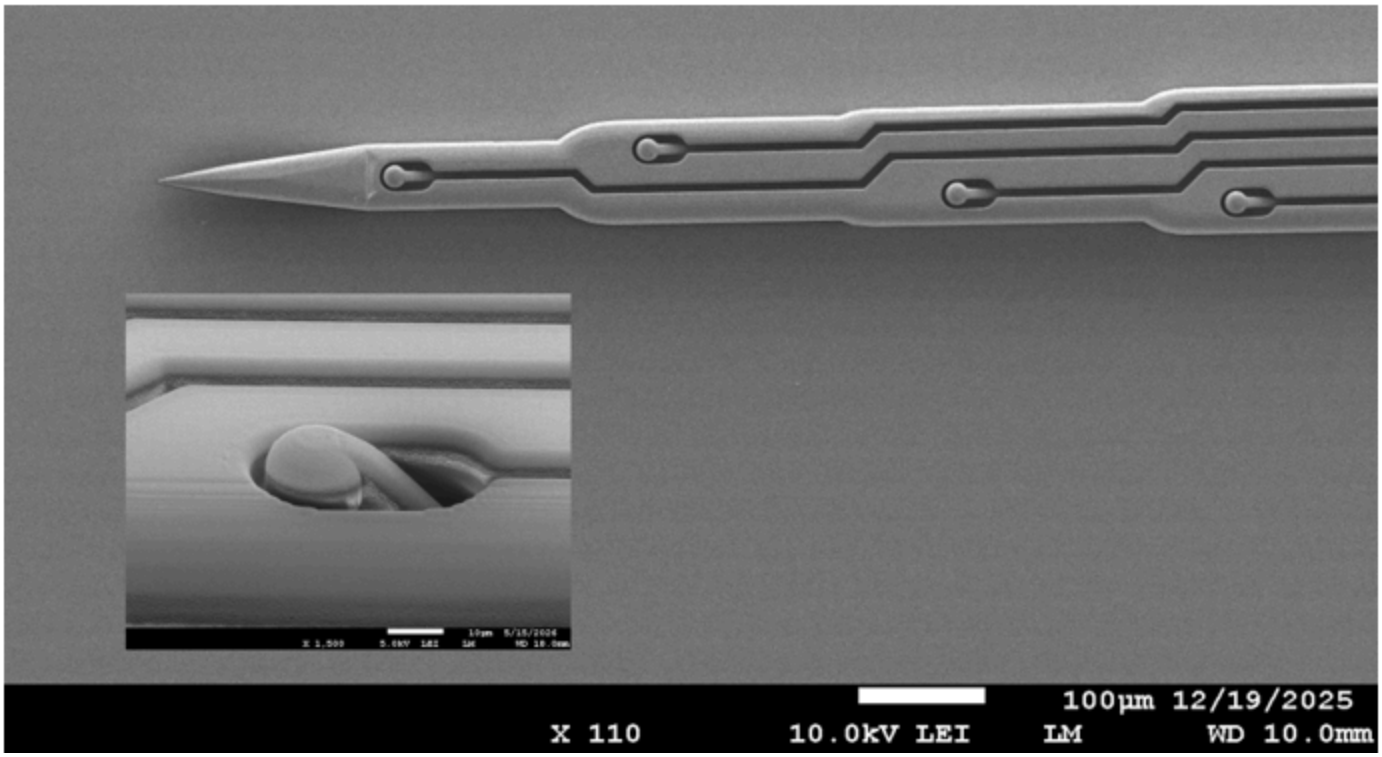


Figure 3

SEM image of the neural probe after Ti/Au metallization. Inset: tilted view of a mushroom-shaped electrode.

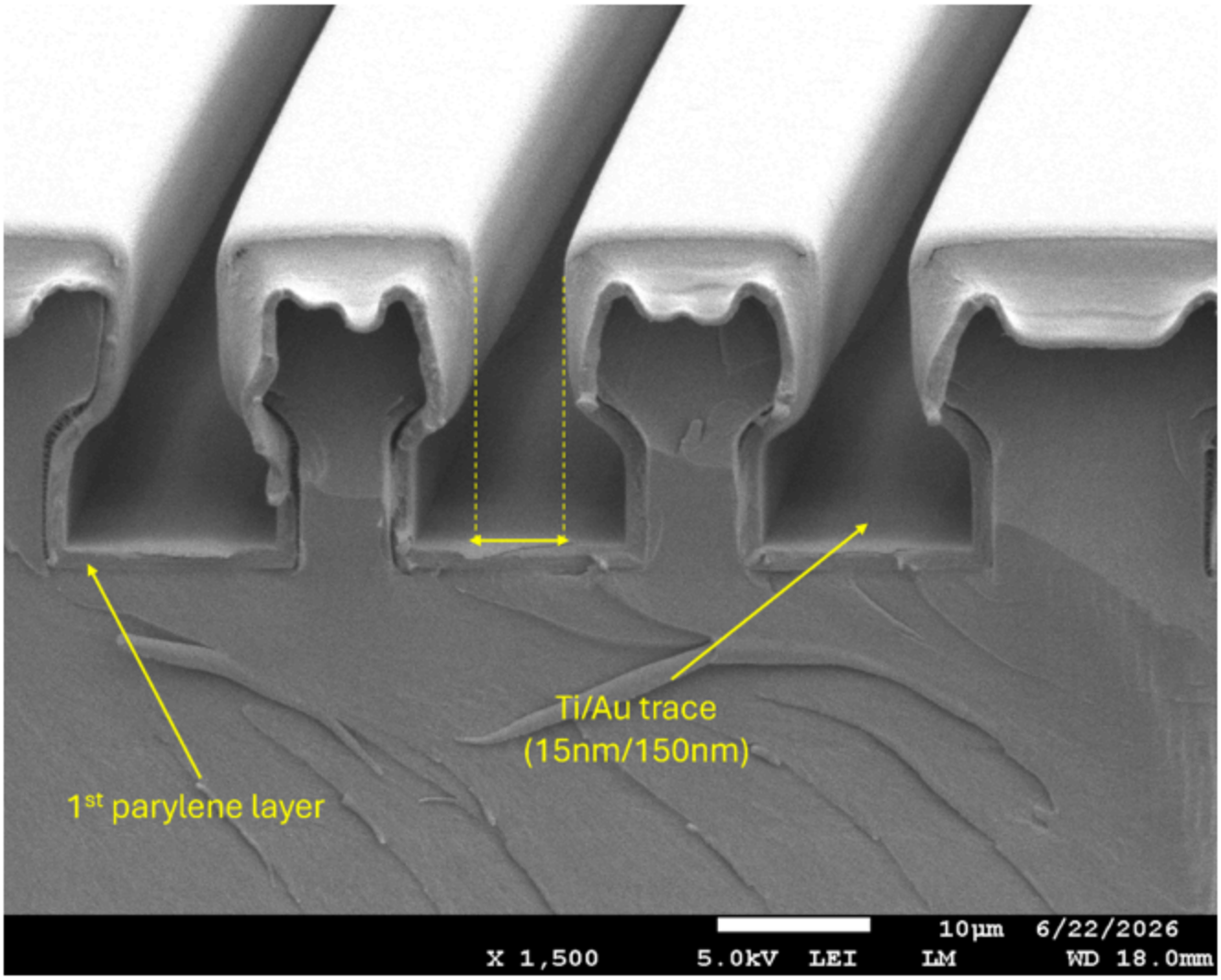


Figure 4

Cross-sectional SEM image after Ti/Au deposition on the 1 µm Parylene-C base layer, showing metal at the bottoms of the re-entrant trenches.

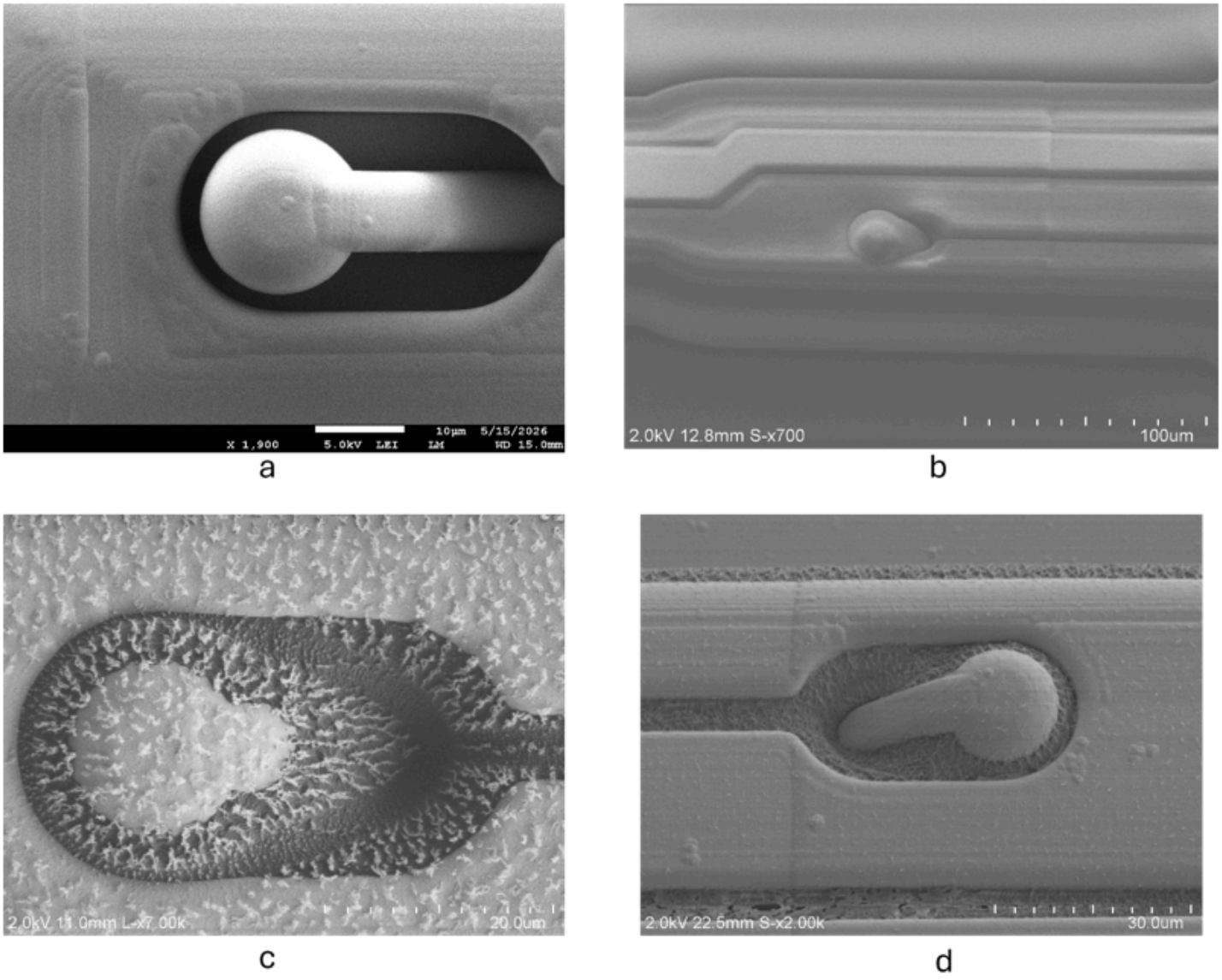


Figure 5

SEM images of the electrode region after (a) Ti/Au metallization, (b) Parylene-C encapsulation (image blurring due to charging), (c) O_2 plasma etch-back, and (d) SF_6/O_2 plasma treatment.

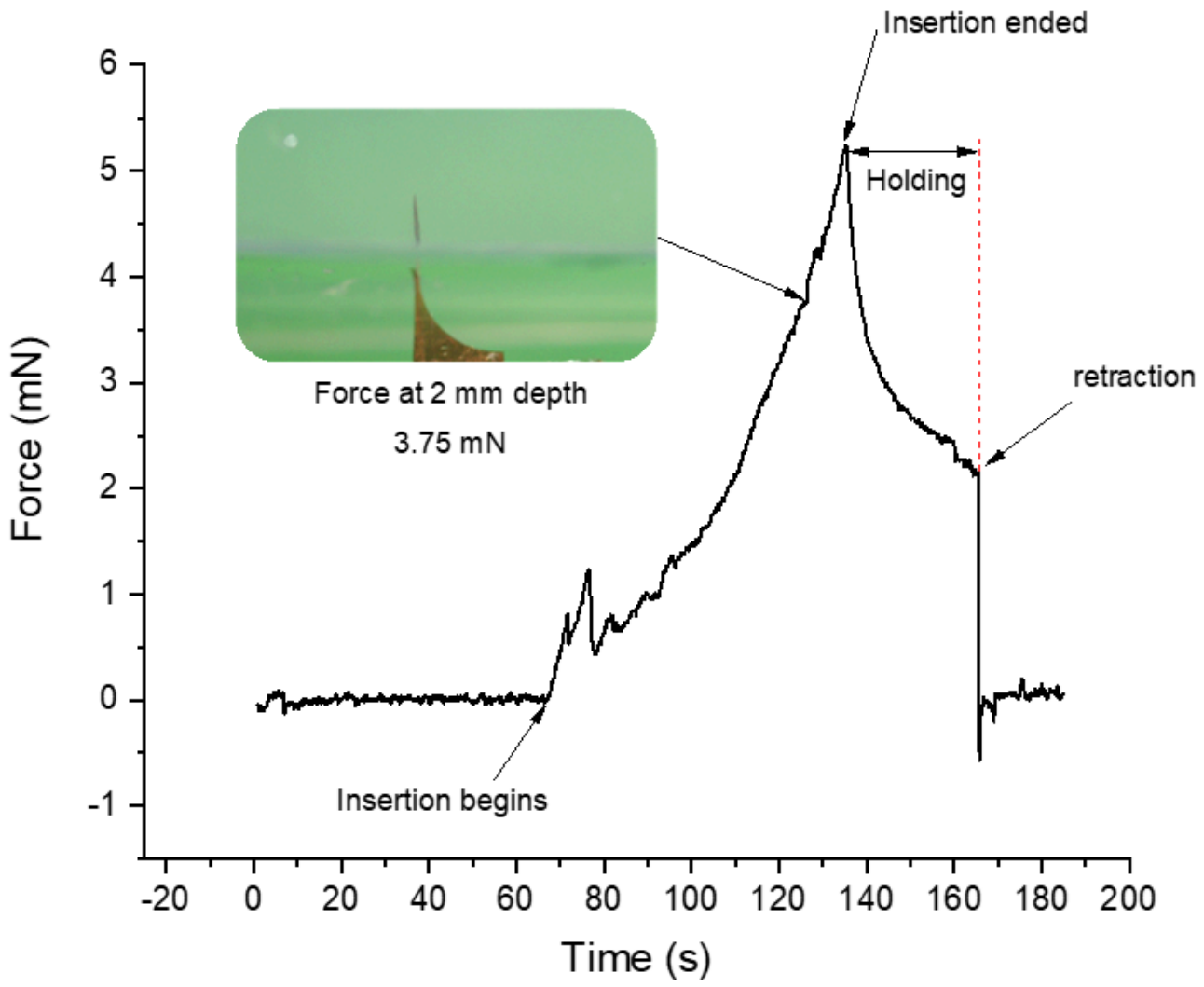


Figure 6

Insertion of the 3D-printed neural probe into 0.6% agarose gel. The force profile shows insertion onset, the end of insertion, a holding period, and retraction, with a force of 3.75 mN at a 2 mm insertion depth. Inset: successful 2 mm shank insertion.

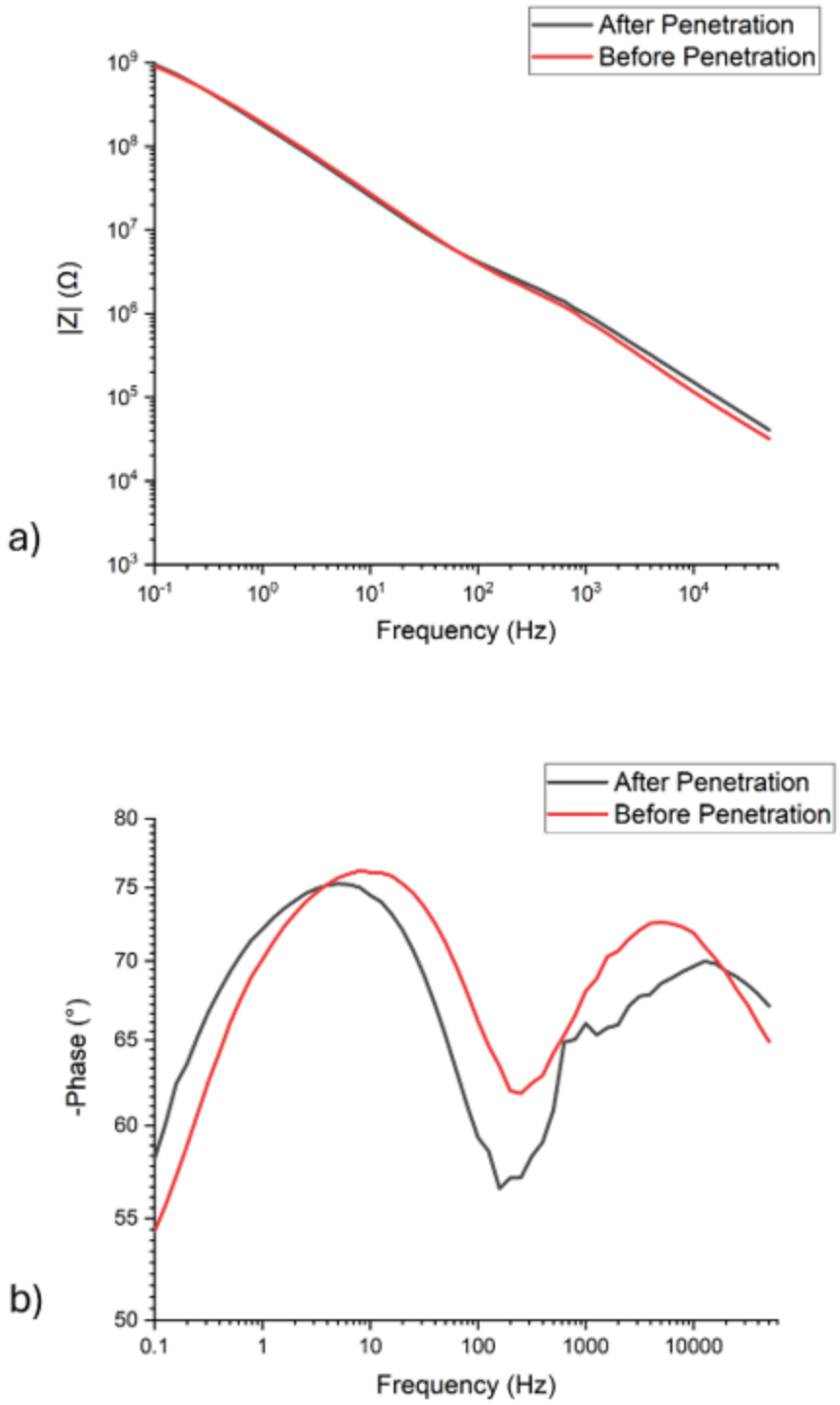


Figure 7

EIS measured in PBS before and after insertion into 0.6% agarose gel: (a) impedance magnitude and (b) negative phase angle (-phase), as plotted.